

Biomechanical Design of a Powered Ankle-Foot Prosthesis

Samuel K. Au, Jeff Weber, and Hugh Herr

Abstract—Although the potential benefits of a powered ankle-foot prosthesis have been well documented, no one has successfully developed and verified that such a prosthesis can improve amputee gait compared to a conventional passive-elastic prosthesis. One of the main hurdles that hinder such a development is the challenge of building an ankle-foot prosthesis that matches the size and weight of the intact ankle, but still provides a sufficiently large instantaneous power output and torque to propel an amputee.

In this paper, we present a novel, powered ankle-foot prosthesis that overcomes these design challenges. The prosthesis comprises an unidirectional spring, configured in parallel with a force-controllable actuator with series elasticity. With this architecture, the ankle-foot prosthesis matches the size and weight of the human ankle, and is shown to be satisfying the restrictive design specifications dictated by normal human ankle walking biomechanics.

I. INTRODUCTION

Today's commercially available below-knee prostheses are completely passive during the stance phase of walking, and consequently their mechanical properties remain fixed with walking speed and terrain. Clinical studies indicate that transtibial amputees using these conventional passive prostheses experience many problems during locomotion, including non-symmetric gait patterns, slower self-selected walking speeds, and higher gait metabolic rates compared to intact individuals [1][2][3]. For example, transtibial amputees expend 20-30% more metabolic power to walk at the same speed as able-bodied individuals, and therefore, they prefer a slower walking speed to travel the same distance [2][3].

There are many mechanical differences between conventional ankle prostheses and the human ankle. Most notably, the human ankle performs more positive mechanical work than negative, especially at moderate to fast walking speeds [4][5][6]. Researchers hypothesize [8][9] that the inability of conventional passive prostheses to provide net positive work over the stance period is the main cause for the above clinical difficulties.

This motivates us to develop a powered ankle-foot prosthesis that is capable of providing sufficient active mechanical power or net positive work during the stance period of walking. We hypothesize that such a device can significantly improve

below-knee amputee ambulation, such as walking symmetry, self-selected walking speed, and walking metabolism.

A. Previous Work

Although the idea of a powered ankle-foot prosthesis has been discussed since the late 1990s, only one attempt [10] has been made to develop such a prosthesis to improve amputee ambulation. Klute [10] attempted to use an artificial pneumatic muscle, called McKibben actuator to develop a powered ankle-foot prosthesis. More recent work has focused on the development of quasi-passive ankle-foot prostheses [11][12][13]. Collins and Kuo [11] advanced a foot system that stores elastic energy during early stance, and then delays the release of that energy until late stance, in an attempt to reduce impact losses of the adjacent leg. Since the device did not include an actuator to actively plantar flex the ankle, no net work was performed throughout stance. Other researchers [12][13] have built prostheses that use active damping or clutch mechanisms to allow ankle angle adjustment under the force of gravity or the amputee's own weight. In the commercial sector, the most advanced ankle-foot prosthesis, the Össur Proprio FootTM [14], has an electric motor to adjust the orientation of a low profile passive-elastic foot during the swing phase. Although active during the swing phase, the Proprio ankle joint is locked during stance, and therefore becomes equivalent to a passive elastic foot. Consequently, no net positive work is done at the ankle joint during stance.

B. Engineering Challenges

There are two main hurdles hinder the development of a powered ankle-foot prosthesis [1][15][16]. First, it is challenging to build an ankle-foot prosthesis that matches the size and weight of the human ankle, but still provides a sufficiently large instantaneous power output and torque to propel an amputee. For example, a 75kg person has an ankle-foot weight equal to approximately 2.5kg, and a peak power and torque output at the ankle during walking as high as 350W and 140Nm, respectively [4][6][15]. Current ankle-foot mechanisms for humanoid robots are not appropriate for this application, as they are either too heavy or not powerful enough to meet the human-like specifications required for a prosthesis [17][18].

Second, there is no clear control target or "gold standard" for the prosthesis to be controlled, against which to gauge the effectiveness. It is unclear what kind of prosthetic control strategy is effective for the improvement of amputee ambulation.

The key objective of this paper is to address the mechanical design challenge of the power ankle-foot prosthesis. We propose a novel, motorized prosthesis that exploits both series and parallel elasticity to fulfill the demanding human-like

This work was performed in the Biomechanics Group at the MIT Media Lab and was supported in part by the U.S Department of Veteran's Administration under Grant V650P-3945.

S. Au is with the Department of Mechanical Engineering and the Media Lab, Massachusetts Institute of Technology, Cambridge, MA 02139 USA (corresponding author phone: 617-324-1701; e-mail: kwau@mit.edu.)

J. Weber is with the Media Lab, Massachusetts Institute of Technology, Cambridge, MA 02139 USA

H. Herr is with the Media Lab and the Harvard-MIT Division of Health Sciences and Technology, Massachusetts Institute of Technology, Cambridge, MA 02139, USA. email: hherr@media.mit.edu

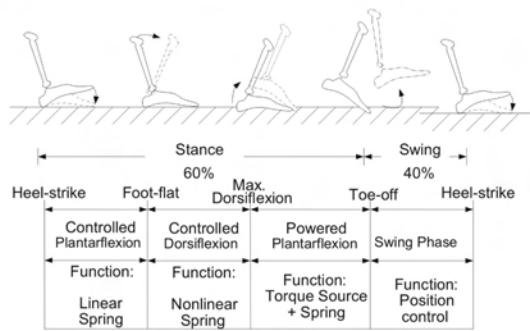


Fig. 1. Normal human ankle walking biomechanics for level-ground walking.

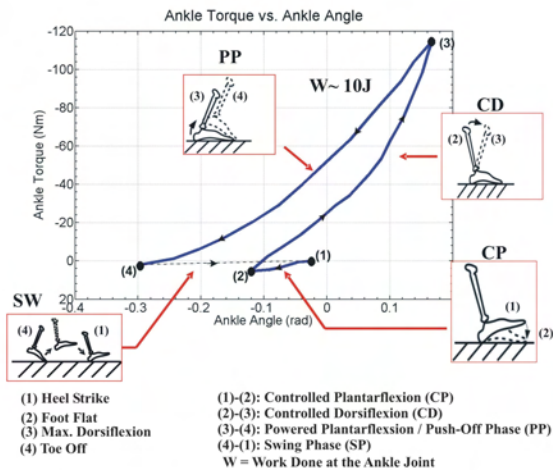


Fig. 2. A typical ankle torque-angle behaviour for a 75 kg person at his/her self-selected walking speed (1.25m/sec). Data are from [6], re-plotted in the manner of [16]. The solid line shows the ankle torque-angle behaviour during stance while the dash line shows the ankle behaviour during the swing phase. The points (1), (2), (3), and (4) represent the conditions of the foot at heelstrike, foot flat, maximum dorsiflexion, and toe-off, respectively. The segments (1)-(2), (2)-(3), (3)-(4), and (4)-(1) represent the ankle torque-angle behaviours during CP, CD, PP, and SW phases of gait, respectively. As can be seen in, segments (1)-(2) and (2)-(3) reveals the different spring behaviors of the human ankle joint during CP and CD, respectively. The area W enclosed by the points (2), (3), and (4) shows the net positive work done at the joint.

specifications required for a prosthesis [4][15]. The control system design challenge and corresponding clinical evaluation have been addressed in [19].

C. Paper Outline

In this paper, we first review the biomechanics of a normal human ankle in walking, and then use this biomechanical study to motivate the prosthetic design. Numerical and experimental studies are conducted to justify the design approach.

II. DESIGN SPECIFICATIONS AND TARGET ANKLE STANCE BEHAVIORS FOR THE PROSTHESIS

In this section, we first review the walking biomechanics of a human ankle in walking. Using these biomechanical descriptions, we define the design specifications and the target ankle stance behaviors for the prosthesis.

A. Normal Human Ankle-Foot Walking Biomechanics

A level-ground walking gait cycle is typically defined as beginning with the heel strike of one foot and ending at the next heel strike of the same foot [20]. The main subdivisions of the gait cycle are the stance phase (60% of a gait cycle) and the swing phase (40% of a cycle). The swing phase (SW) represents the portion of the gait cycle when the foot is off the ground. The stance phase begins at heel-strike when the heel touches the floor and ends at toe-off when the same foot rises from the ground surface. From [5][6], the stance phase of walking can be divided into three sub-phases: Controlled Plantar Flexion (CP), Controlled Dorsiflexion (CD), and Powered Plantar Flexion (PP). Fig. 2 shows the typical ankle torque-angle characteristics for a 75kg person walking at his/her self-selected speed (1.25m/sec). The detailed descriptions for each sub-phase are provided below.

CP begins at heel-strike and ends at foot-flat. During CP, the ankle behavior is consistent with a linear spring response [5][6]. The segment (1)-(2) in Fig. 2 illustrates the linear spring behavior of the ankle.

CD begins at foot-flat and continues until the ankle reaches a state of maximum dorsiflexion. During CD, the ankle behavior can be described as a nonlinear spring for energy storage [5]. Segment (2)-(3) in Fig. 2 reveals the nonlinear spring behavior of the human ankle joint during CD.

PP begins after CD and ends at the instant of toe-off. During PP, the ankle can be modeled as a torque source in parallel with the CD spring. The area W enclosed by the points (2), (3), and (4) shows the net work done at the ankle.

SW begins at toe-off and ends at heel-strike. During SW, the ankle can be modeled as a position source to reset the foot to a desired equilibrium position before the next heel strike.

In summary, for level ground walking, human ankle provides three main functions: (i) it behaves as a spring with variable stiffness from CP to CD; (ii) it provides additional energy for push-off during PP; and (iii) it behaves as a position source to control the foot orientation during SW.

B. Target Stance Phase Behavior

Referring to Section I-B, the key question for the control is to define/design a target walking behavior for the prosthesis. For the swing phase, the desired behavior is just to re-position the foot to an predefined equilibrium position. For the stance phase control, instead of simply tracking ankle kinematics, it is commonly believed that the best way is to let the prosthesis mimic the "quasi-static stiffness", that is the slope of the measured ankle torque-angle curve during stance [5][6]. Mimicking the quasi-static stiffness curve of an intact ankle during walking (Fig. 2) is the main goal for the stance phase control.

As can be seen in Fig. 3(A), a typical quasi-static stiffness curve can be decomposed into two main components: (1) a

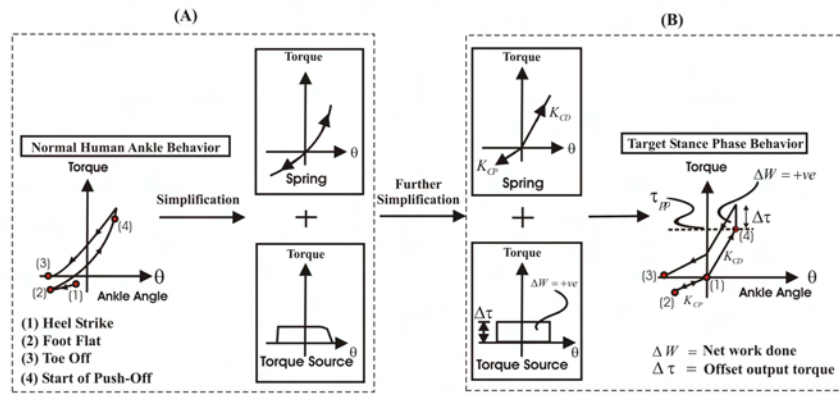


Fig. 3. Target stance phase behavior. The normal human ankle behavior (quasi-static stiffness curve) was decomposed into a spring component and a torque source. The spring component was then piecewise linearized and its stiffness varies with the sign of the ankle angle. The torque source was modeled as a constant offset torque $\Delta\tau$, which was applied to the ankle joint from points (4) to (3).

spring whose stiffness varies in a similar manner to the normal human ankle does in CP and CD. (2) a torque source that provides positive net work during late stance phase. For the ease of implementation, we modified these two components to obtain the target stance phase behavior as depicted in Fig. 3(B). Each component is described as follows:

- 1) A linear torsional spring with a stiffness that varies with the sign of the ankle angle. When the ankle angle is positive, the stiffness value will be set to K_{CD} . When the ankle angle is negative, the stiffness value will be set to K_{CP} .
- 2) A constant offset torque $\Delta\tau$ is used to model the torque source during PP. This offset torque is applied in addition to the torsional spring K_{CD} during PP. τ_{pp} determines the moment at which the offset torque is applied, indicated by the point (4) in Fig. 3.

It is noted that the conventional passive prostheses only provide the spring behavior but fail to supply the function of the torque source to propel the body during PP. Our designed prosthesis eventually will provide both functions during stance.

C. Design Specifications

Using the above biomechanical descriptions and the results from [5][6][20], the design goals for the prosthesis are summarized as follows:

- the prosthesis should be at a weight and height similar to the intact limb.
- the system must deliver a large instantaneous output power and torque during push-off.
- the system must be capable of changing its stiffness as dictated by the quasi-static stiffness of an intact ankle.
- the system must be capable of controlling joint position during the swing phase.
- the prosthesis must provide sufficient shock tolerance to prevent any damage in the mechanism during the heel-strike.

The corresponding parameters values of the above design goals are given in Table I. These parameters values are

estimated based on the human data from [5][6][20].

TABLE I
DESIGN SPECIFICATIONS

Weight (kg)	2.5
Max. Allowable Dorsiflexion (deg)	15
Max. Allowable Plantarflexion (deg)	25
Peak Torque (Nm)	140
Peak Velocity (rad/s)	5.2
Peak Power (W)	350
Torque Bandwidth (Hz)	3.5
Net Work Done (J)	10J at 1.3m/s
Offset Stiffness (Nm/rad)	550

III. MECHANICAL DESIGN

The basic architecture of our mechanical design is a physical spring, configured in parallel to a high power output force-controllable actuator (Fig. 4). The parallel spring and the force-controllable actuator serve as the spring component and the torque source in Fig. 3(B), respectively. The prosthetic ankle-foot system requires a high mechanical power output as well as a large peak torque. The parallel spring shares the payload with the force-controllable actuator, thus the required peak force from the actuator system is significantly reduced. Consequently, a smaller transmission ratio can be used, and a larger force bandwidth is obtained. The series elasticity is also an important design feature for the ankle-foot prosthesis as it can prevent damage to the transmission due to shock loads during heel-strike.

As can be seen in Fig. 4(a), there are five main mechanical elements in the system: a high power output d.c. motor, a transmission, a series spring, a unidirectional parallel spring, and a carbon composite leaf spring prosthetic foot. The first three components are combined to form a force-controllable actuator, called Series-Elastic Actuator(SEA). A SEA, previously developed for legged robots [21], consists of a dc motor in series with a spring (or spring structure) via a mechanical transmission. The SEA provides force control by controlling the extent to which the series spring is compressed. Using a

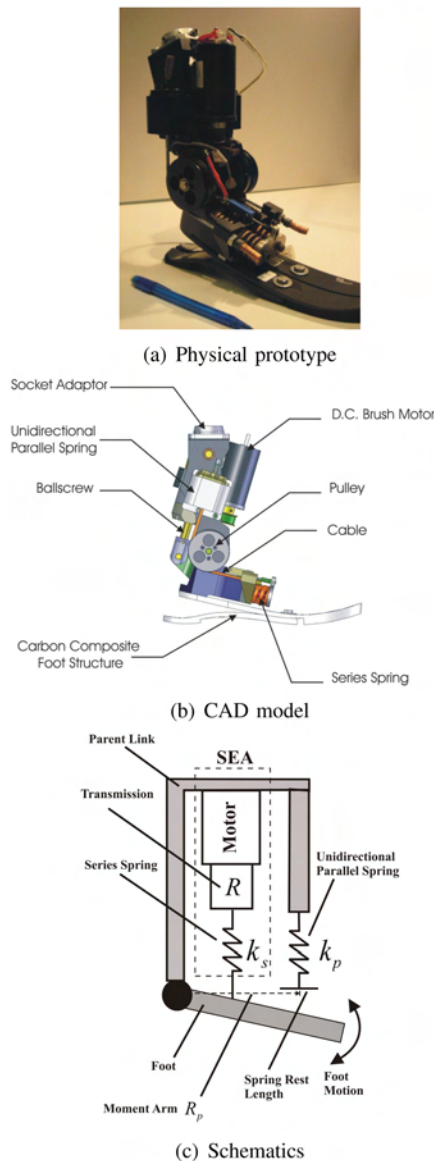


Fig. 4. Mechanical design of the prosthesis.

linear potentiometer, we can obtain the force applied to the load by measuring the deflection of the series spring.

In this application, we use the SEA to modulate the joint stiffness as well as provide the constant offset torque $\Delta\tau$. The SEA provides a stiffness value K_{CP} during CP and a stiffness value K_{CD1} from CD to PP (Fig. 5). From points (4) to (3), it supplies both the stiffness value K_{CD1} and a constant, offset torque $\Delta\tau$.

Due to the demanding output torque and power requirements, we incorporate a physical spring, configured in parallel to the SEA, so that the load borne by the SEA is greatly reduced. Because of this fact, the SEA will have a substantially large force bandwidth to provide the active push-off during PP. To avoid hindering the foot motion during swing phase, the parallel spring is implemented as an unidirectional spring that provides an offset rotational stiffness value K_p^r only when the

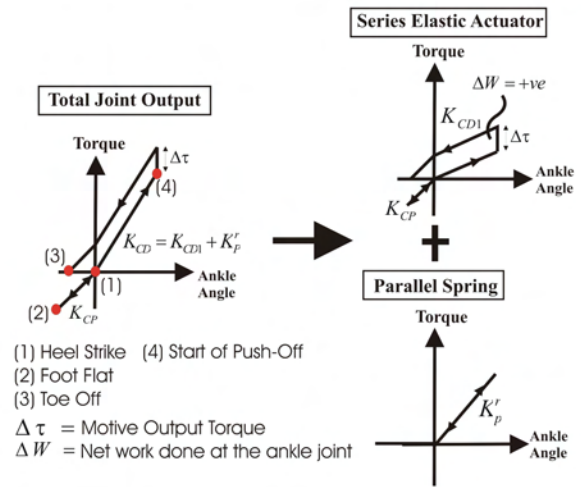


Fig. 5. Exploiting the parallel and series elasticity with an actuator. The parallel spring provides a biased, offset stiffness K_p^r when the ankle angle is larger than zero degree. The series spring combined with the actuator, so called an SEA [21], is used to modulate the joint stiffness and serve as a torque source to do positive work at the ankle joint.

ankle angle is larger than zero degree (Fig. 5).

The elastic leaf spring foot is used to emulate the function of a human foot that provides shock absorption during foot strike, energy storage during the early stance period, and energy return in the late stance period. A standard prosthetic foot, Flex Foot LP Vari-Flex [14] is used in the prototype.

A. Component Selections

Broadly speaking, there are three main design decisions in this project: (1) choosing the parallel spring stiffness, (2) choosing the actuator and transmission, and (3) choosing the series spring stiffness.

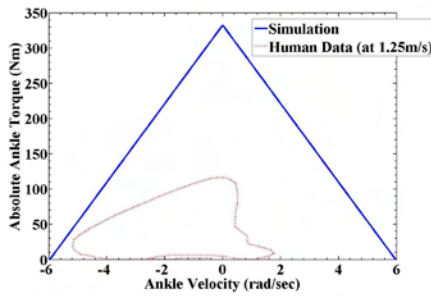
1) *Parallel Spring*: A linear parallel spring k_p with a moment arm R_p in Fig. 4(c) provides a rotational joint stiffness K_p^r ,

$$K_p^r = (k_p)(R_p)^2 \quad (1)$$

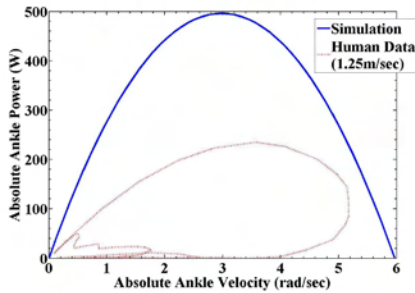
The goal is to properly select the moment arm and the spring constant in order to provide the suggested offset stiffness in Table I. In the physical system, due to the size and weight constraints, k_p and R_p were chosen to be 770KN/m and 0.022m, respectively. Consequently, $K_p^r=385\text{rad/s}$. Because this value is smaller than the suggested offset stiffness(550rad/s), the SEA supplements the required joint stiffness (see Fig. 5).

2) *Actuator and Transmission*: The goal is to select an actuator and a transmission to bracket the maximum torque and speed characteristics of the prosthesis, so as to match the intact ankle torque/power-speed requirements (Fig. 6).

In our design, a 150W d.c. brushed motor from Maxon, Inc (RE-40) was used because its peak power output(500W) is much larger than that of the human ankle in walking (350W). For the drive train system, the motor drives a 3mm pitch linear ballscrew via a timing-belt drive transmission with a 1.7:1 ratio. The translational movement of the ballscrew causes



(a) Absolute Joint Torque vs. Joint Velocity



(b) Absolute Joint Power vs. Absolute Joint Velocity

Fig. 6. Comparisons of the joint torque/power-speed characteristic of the prosthesis to that of the normal human ankle during walking.

an angular rotation of the ankle joint via a moment arm $r=0.0375\text{m}$ and the series spring.

Assuming the series spring will be chosen to be very stiff, the total transmission ratio $R_{total} \sim 133$ was selected, where R_{total} is defined as the ratio of the input motor velocity to the output ankle joint velocity. The peak torque/speed characteristics of the prosthesis in Fig. 6 has shown that the prosthesis is capable to generating normal human ankle-foot walking behavior. Furthermore, the power output characteristics of the prosthesis were designed to match that of the intact ankle during walking.

3) *Series Spring*: According to [21], the selection criteria for the series spring is mainly based on the large force bandwidth because the series elasticity substantially reduces the system bandwidth at large force due to the motor saturation. The stiffer the spring is, the higher the SEA bandwidth is at large force. Therefore, by choosing a stiffer spring, our design goal was to have the large force bandwidth of the SEA much greater than the required force bandwidth in the specifications (Table I).

To analyze the large force bandwidth, we proposed a simple linear model (Fig. 7) for the prosthesis based on [21]. All system parameters and variables were converted to the linear motion of the ballscrew in the prosthesis. We define a transmission ratio R that converts rotary motion of the motor into linear compression on the series spring (See Fig. 4(c)). The effective motor mass M_e , damping B_e , and linear motor force F_e can be obtained using the following equations: $M_e = I_m R^2$, $F_e = T_m R$, $B_e = b_m R$, where I_m , T_m , b_m are the rotary motor inertia, motor torque, the damping term of the motor,

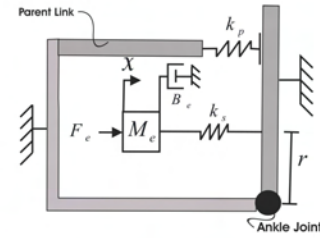


Fig. 7. A simple linear model of the prosthesis for the bandwidth analysis. All degrees of freedom are transferred to the translation domain of the ballscrew. M_e , B_e , and F_e represent the effective mass, damping, and linear motor force acting on effective mass, respectively, while x and k_s are the displacement and the spring constant of the series spring.

TABLE II
MODEL PARAMETERS

Parameters	F_{sat}	V_{sat}	M_e	B_e
Values	7654N	0.23m/s	170kg	8250Ns/m

respectively. Both ends of the prosthesis are fixed for the bandwidth analysis, consequently, the equation of motion for this model becomes a standard second-order differential equation for a spring-mass-damper system. The spring force F_s was considered as the system output. According to [21], the large force bandwidth is defined as the frequency range over which the actuator can oscillate at a force amplitude F_s^{max} due to the maximum input motor force, F_{sat} . The transfer function that describes the large force bandwidth is:

$$\frac{F_s^{max}}{F_{sat}} = \frac{k_s}{M_e s^2 + (B_e + \frac{F_{sat}}{V_{sat}})s + k_s} \quad (2)$$

where F_s^{max} , V_{sat} are the maximum output force and maximum linear velocity of the motor respectively. They are defined as $F_{sat} = RT_{motor}^{max}$ and $V_{sat} = \frac{\omega_{motor}^{max}}{R}$. As can be seen in (2), the large force bandwidth is independent of the control system, but rather depends on the intrinsic system behaviors which are determined by the choices of the motor, transmission ratio, and the spring constant.

In our design, the total spring constant for the series springs is set to 1200KN/m. Using the motor parameters (Maxon RE-40) in [22] and transmission ratio ($R=3560$), the model parameters were obtained and shown in Table II. The simulation result for the large force bandwidth has shown in Fig. 8.

As shown in Fig. 8, the estimated large force bandwidth of the system with and without the parallel spring was at 9.4Hz (at 50Nm) and 3.8Hz (at 120Nm), respectively. As the parallel spring shared some of the payloads of the SEA, the required peak force for the system was significantly reduced. With the parallel spring, the estimated force bandwidth were much larger than the designed criteria in Table I. In practice, it is favorable to design a system whose large force bandwidth is several times larger than the required bandwidth as there are many factors that can substantially reduce the large force bandwidth, such as unmodeled friction [21].

We also conducted open-loop bandwidth tests for the system by applying a chirp signal as the desired input command for the controller. The result for the bandwidth test is shown

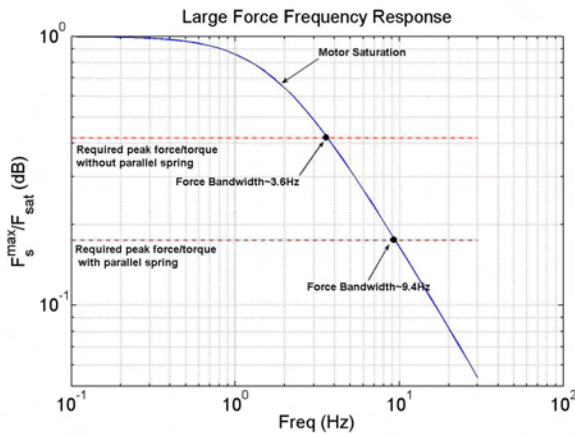


Fig. 8. Simulation result for the large force bandwidth due to motor saturation. A relatively stiffer series spring was used to obtain greater large force bandwidth.

in Fig. 9. In general, the experimental result matched with the simulation of the spring-mass-damper system. The force bandwidth of the system using an input force $F_e = 800N$ (or input torque $T = 30Nm$) was about 14Hz. As can be seen, the experimental frequency response curve dropped off rapidly at high frequency, mainly due to the motor and amplifier saturation. It also appeared that there was an unmodeled zero at low frequency.

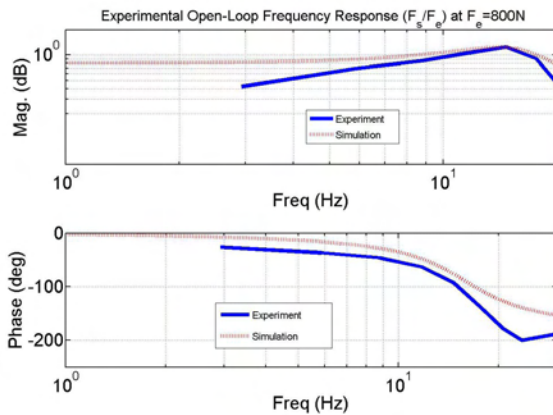


Fig. 9. Experimental open-loop frequency response.

Again, the above bandwidth analysis was used for the design purpose that provided a guideline for the selection of the series spring. For a better prediction of the actual system behavior, an advanced system model needs to be proposed. In [19], we had shown that the proposed biomimetic mechanical design allowed the control system to mimic normal human ankle walking behavior. The pilot clinical studies supports the hypothesis that a powered ankle-foot prosthesis that mimics normal human ankle stance phase behavior can improve an amputee's gait.

IV. CONCLUSION

In this paper, a novel, powered ankle-foot prosthesis is proposed. The prosthesis comprises an unidirectional spring in parallel with a high performance, force-controllable actuator with series elasticity. By exploiting both parallel and series elasticity, the design is shown to be capable of satisfying the restrictive design specifications dictated by normal human ankle walking biomechanics.

ACKNOWLEDGMENT

The authors wish to thank E. C. Martinez and B. Deffenbaugh for their contributions in mechanical and circuit designs.

REFERENCES

- [1] D. A. Winter and S. E. Sienko, "Biomechanics of below-knee amputee gait," *Journal of Biomechanics*, Vol. 21, No. 5, pp. 361-7, 1988.
- [2] N. H. Molen, "Energy/speed relation of below-knee amputees walking on motor-driven treadmill," *Int. Z. Angew. Physio*, Vol. 31, pp.173, 1973.
- [3] G. R. Colborne, S. Naumann, P. E. Longmuir, and D. Berbrayer, "Analysis of mechanical and metabolic factors in the gait of congenital below knee amputees," *Am. J. Phys. Med. Rehabil.*, Vol. 92, pp. 272 - 278, 1992.
- [4] D. A. Winter, "Biomechanical motor pattern in normal walking," *Journal of Motor Behavior*, Vol. 15, No. 4, pp. 302 - 330, 1983.
- [5] M. Palmer, "Sagittal plane characterization of normal human ankle function across a range of walking gait speeds," *Master's Thesis*, Massachusetts Institute of Technology, 2002.
- [6] D. H. Gates, "Characterizing ankle function during stair ascent, descent, and level walking for ankle prosthesis and orthosis design," *Master's thesis*, Boston University, 2004.
- [7] A. D. Kuo, J. M. Donelan, and A. Ruina, "Energetic consequences of walking like an inverted pendulum: Step-to-step transitions," *Exercise and Sport Sciences Reviews*, Vol. 33, pp. 88-97, 2005.
- [8] A. Ruina, J. E. Bertram, and M. Srinivasan, "A collisional model of the energetic cost of support work qualitatively explains leg sequencing in walking and galloping, pseudo-elastic leg behavior in running and the walk-to-run transition," *Journal of Theoretical Biology*, Vol. 237, Issue 2, pp. 170-192, 2005.
- [9] G. K. Klute, J. Czerniecki, and B. Hannaford, "Development of powered prosthetic lower limb," *Proc. 1st National Mtg. Veterans Affairs Rehab. R&D Service*, Washington, DC, October 1998.
- [10] S. H. Collins and A. D. Kuo, "Controlled energy storage and return prosthesis reduces metabolic cost of walking," *Proc. on ISB XXth Congress and the American Society of Biomechanics Annual Meeting*, Cleveland, Ohio, pp. 804, August 2003.
- [11] C. Li, et al., "Research and development of the intelligently-controlled prosthetic ankle joint," *Proc. of IEEE Int. Conf. on Mechatronics and Automation*, Luoyang, China, pp. 1114-1119, 2006.
- [12] US Patent 6443993, Sept. 3, 2002.
- [13] www.ossur.com.
- [14] K. Koganezawa, and I. Kato, "Control aspects of artificial leg," *IFAC Control Aspects of Biomedical Engineering*, pp.71-85, 1987.
- [15] S. K. Au, P. Dilworth, and H. Herr, "An ankle-foot emulator system for the study of human walking biomechanics," *Proc. IEEE Int. Conf. on Robotics and Automation*, Orlando, FL, pp. 2939-2945, May 2006.
- [16] K. Hirai, et al., "The development of Honda humanoid robot," *Proceedings on IEEE/RSJ International Conference on Intelligent Robots and Systems*, Leuven, Belgium, pp. 1321-1326, May 1998.
- [17] K. Kaneko, et al., "Humanoid robot HRP-2," *Proc. IEEE Int. Conf. on Robotics and Automation*, New Orleans, LA, pp. 1083-1090, April 2004.
- [18] S. K. Au, "Powered Ankle-Foot Prosthesis for the Improvement of Amputee Walking Economy," *Ph.D. Thesis*, Massachusetts Institute of Technology, 2007.
- [19] V. T. Inman, H. J. Ralston, and F. Todd, *Human walking*. Baltimore: Williams and Wilkins; 1981.
- [20] D. Robinson, "Design and an analysis of series elasticity in closed-loop actuator force control," *Ph.D. Thesis*, Massachusetts Institute of Technology, 2000.
- [21] www.maxon.com